

Conductivity of Si(111)-(7 × 7): The Role of a Single Atomic Step

Bruno V. C. Martins,^{1,2} Manuel Smeu,³ Lucian Livadaru,⁴ Hong Guo,³ and Robert A. Wolkow^{1,2,*}

¹National Institute for Nanotechnology, National Research Council of Canada, Edmonton, Alberta, Canada T6G2M9

²Department of Physics, University of Alberta, Edmonton, Alberta, Canada T6G 2E1

³Centre for the Physics of Materials and Department of Physics, McGill University, Montreal, Quebec, Canada H3A2T8

⁴Quantum Silicon Inc., Edmonton, Alberta, Canada T6G 2M9

(Received 3 October 2013; revised manuscript received 17 December 2013; published 18 June 2014)

While it is known that the Si-(7 × 7) is a conducting surface, measured conductivity values differ by 7 orders of magnitude. Here we report a combined STM and transport method capable of surface conductivity measurement of step-free or single-step containing surface regions and having minimal interaction with the sample, and by which we quantitatively determine the intrinsic conductivity of the Si-(7 × 7) surface. We found that a single step has a conductivity per unit length about 50 times smaller than the flat surface. Our first principles quantum transport calculations confirm and lend insight into the experimental observation.

DOI: 10.1103/PhysRevLett.112.246802

PACS numbers: 73.25.+i, 68.37.Ef, 73.63.-b

The Si(111)-(7 × 7) surface has been extensively investigated for decades because of its complex reconstruction and fascinating electronic properties [1]. While bulk Si is a semiconductor with an intrinsic band gap, its 7 × 7 surface exhibits metallic properties [2,3]. This is due to the adatoms on the surface possessing partially occupied dangling bonds, which form a band that crosses the Fermi level. There have been many experimental attempts to determine the sheet conductivity of this important surface but a consensus has not been reached despite nearly two decades of work. Given the dominating role of Si in micro- and nanotechnology, it is indeed surprising that such a basic property as the surface conductivity has evaded consistent measurements for so long. With the continued downscaling of electronic devices and the advent of nanoelectronics [4,5], quantitative understanding of surface physics becomes very important and the Si(111)-(7 × 7) surface serves as an excellent testing ground for electron transport at the atomic scale.

So far the surface conductivity of Si-(7 × 7) has been measured by single tip scanning tunneling microscope (STM), two-point probe (2PP), four-point probe (4PP), and by electron-energy loss spectroscopy (EELS). While EELS reported a value of $3 \times 10^{-4} \Omega^{-1} \square^{-1}$ [2], the STM and multiprobe measurements yielded many different values including $10^{-4} \Omega^{-1} \square^{-1}$ [6], $10^{-6} \Omega^{-1} \square^{-1}$ [3,7], $4 \times 10^{-6} \Omega^{-1} \square^{-1}$ [8], $9 \times 10^{-9} \Omega^{-1} \square^{-1}$ [9,10] and $9 \times 10^{-11} \Omega^{-1} \square^{-1}$ [11]. The dramatic differences between these values could be due to many factors such as the measurement methods being EELS, 2PP, or 4PP, the distance between the measuring probes being macro or micro, the doping levels of the Si, the measured nanostructures and quality of samples, as well as the presence or absence of atomic steps in between the measuring probes [12,13]. While 4PP is the fundamental technique for

transport measurements, it is not capable of achieving high spatial resolution due to the heavy geometrical constraints imposed by the probe size. To date that approach has not been used to discern the resistance of a single atomic step, although it has revealed that the surface atomic steps are crucially affecting the measured sheet conductivity [13,14]. In any event, with the experimentally reported values spanning 7 orders of magnitude [8,15], quantitative understanding of the electronic conduction in Si-(7 × 7) remains an unresolved problem and it is the purpose of this work to fill this gap.

We have developed a multiprobe technique for high spatial resolution spectroscopy based on a combination of STM and electronic transport measurements. The conductance of a single atomic step can be quantitatively determined and compared with that of the surface having no atomic step at all. This way, we obtain not only the intrinsic sheet conductivity of the 7 × 7 surface but also that an atomic step has, per unit length, a conductivity about 50 times less than a flat surface. Since this is the first time that the resistance of a single atomic step on the Si(111)-(7 × 7) reconstructed surface has been determined by transport measurement, our results suggest that the dramatic differences in the reported sheet conductivity of the 7 × 7 may be due to the presence of an unknown number of atomic steps between the measuring points. By carrying out first principles transport simulations we have calculated the effects of a single atomic step on Si(111)-(7 × 7), and the results confirm the observation that a single step has a dramatic effect on the sheet conductivity. Our measured sheet conductivity of the step-free Si(111)-(7 × 7) surface is $(1.3 \pm 0.3) \times 10^{-6} \Omega^{-1} \square^{-1}$, which is located at the high value side of the reported spectrum of data.

We carried out the experiment using our homemade room-temperature multiprobe [16] instrument which

comprises three independent STMs: two side probes (L and R), which contact the surface as current terminals, and a central probe (C) used for imaging and for voltage measurements. The three probe instrument is capable of emulating four-probe measurements by using two fixed probes and sequentially measuring voltages at different surface positions using a third probe referenced to the common ground. A novel method was developed for noncontact voltage measurement using height-bias (ZV) spectroscopy [17,18]. This approach, which was adapted from the set of established STM spectroscopic techniques, consists of monitoring the tip height as a function of the sweeping bias while the control loop is kept closed. At some point during the tip voltage sweep, the sweeping bias on the tip will match the sample potential, causing the tip to get very close to the surface to compensate for the reduction in current. It is straightforward to note that the ZV spectrum will present a dip corresponding to the surface voltage. It is notable that measurement of the local potential was possible without contact. This is a great advantage since we can move the tip around and construct high spatial resolution and nondestructive maps of the local potential at the surface. This method has some similarity with the original scanning tunneling potentiometry [19] but uses a simpler dc bias procedure.

We now describe the experimental approach in detail. Using two side probes labeled L and R to touch the surface and establish a potential gradient, a current flows in between them. It is required that the contact resistance of both probes be the same and constant with time. This was achieved by using STM proportional-integral control of each of the probes in order to keep the current constant while in contact. As shown in Fig. 1(a), we applied the same control system (one for each probe) used for the STM mode to control the contact. While keeping the sample grounded, we applied a common 2 V bias to both L and R probes (by using a floating preamplifier configuration) and established a $2\ \mu\text{A}$ set point for the current. Using this configuration, it was possible to maintain both L and R probes with a constant contact resistance indefinitely.

Figure 1(b) shows the steps taken during the measurement process: (i) control loops of both L and R probes are turned off and the sample is disconnected from ground; (ii) a potential gradient is applied between the L , R probes; (iii) The C probe enters in the tunneling regime; (iv) ZV spectroscopy measures the sample local potential; (v) the C probe is retracted and moved to the next measurement position; (vi) the sample is reconnected to the ground and the control loops of both side probes are reconnected. The entire process takes only a few seconds allowing us to disregard contact variations during the measurement.

We applied this technique to measure the conductivity of both a step-free surface and a surface region containing a single monatomic step on Si-(7×7). We performed experiments using n -type samples with nominal resistivity of

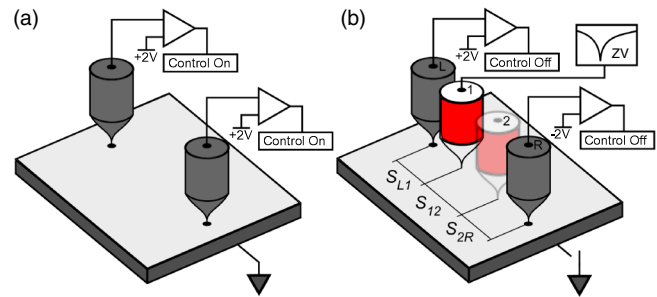


FIG. 1 (color online). (a) Contact control using the STM proportional-integral loop with a $2\ \mu\text{A}$ setpoint. Both probes have bias set to +2 V while the sample is grounded. (b) Acquisition of the potential profiles. Control loops of the two side probes (L and R) are turned off, the sample is disconnected from the ground and a potential difference of 4 V is established. A current now flows between L and R and the central probe enters in STM mode for the acquisition of the ZV spectra. After acquisition, the central probe is retracted and the system returns to the condition presented in (a). The potential profile is constructed by repeating this same process at many points along a straight line defined in the STM scan frame. Labels 1 and 2 correspond to the extreme points of the potential profile.

$1\text{--}3\ \Omega\text{cm}$. By fixing the L and R probes on the sample surface and applying a total bias voltage of 4 V ($L = -2\ \text{V}$, $R = +2\ \text{V}$), we record the ZV spectra by the central probe C at multiple points along the surface [see Fig. 1(b)]. Figure 2(a) shows four recorded typical ZV curves versus the potential of probe C for a surface with a single atomic step, each curve at a unique surface position as indicated by the colored symbols in Fig. 2(b). Each point in Fig. 2(b), was calculated from an average of 10 ZV spectra. The most prominent feature of the ZV curves is the very sharp dip, the position of which gives a measure of the local sample potential as discussed above. Measurements traversing a single atomic step are plotted in Fig. 2(b). A most important finding is the steplike jump (indicated by the up arrow) in the voltage profile which correlated well with the STM step topography (inset and Ref. [20]). We observe that, due to surface conduction from L to R , the resistance of a single atomic step creates a potential jump which our experiment measures unambiguously.

To further confirm that the potential jump was indeed due to surface conduction, we acquired another potentiometric curve [see Fig. 2(b)]: this time on a sample dosed for 50 s at 10^{-6} Torr with 1,2,4-Trimethylbenzene. The adsorbed molecules used to eliminate dangling bonds are not expected to dope or otherwise affect the interface to create a new conduction pathway, as discussed more fully in the Supplemental Material [20]. By STM imaging, we found that such a dose reacts with most of the surface dangling bonds, thus reduces (or eliminates) the surface conduction mechanism. Indeed, we observe an increase in slope compared to that for the clean (undosed) sample and the potential jump has disappeared. The disappearance of

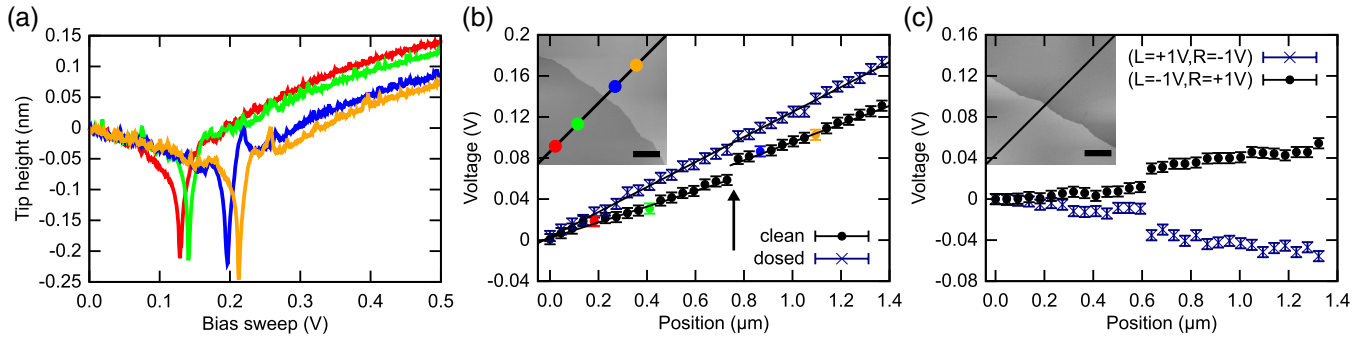


FIG. 2 (color online). (a) ZV spectra collected at different positions on the diagonal. (b) Potential profile acquired on both clean and dosed (50 L 1,2,4-Trimethylbenzene) surfaces. The clean profile displays the fitting function used to calculate the conductivity. The potential difference is 4 V. Inset: STM image showing the diagonal along the $[11\bar{2}]$ direction, where the profile was acquired, and the monatomic step edge. Some points are identified by colors that match the corresponding potential profile displayed in (a). (c) Potential profile acquired on a clean sample with potential difference 2 V and with inverted polarities. Note the mirroring of the profile and the scaling of the voltage by a factor of approximately 2. All scale bars = 200 nm.

the potential jump indicates the loss of a surface-state conduction channel. The overall increase in slope after dosing the silicon dangling bonds corresponds to a net decrease of conduction. After dosing, only the relatively resistive space charge layer and bulk Si remain available for conduction.

By reversing the polarity of the bias voltage applied to the L and R probes, the potential drop also reverses as shown in Fig. 2(c). Such an inversion of the voltage jump and the slope confirms that the observed physical feature (e.g., the potential jump) is not topographical in origin but from conduction on the surface. Measurements were also carried out on a highly doped sample [20].

Having established that the potential jump is due to the single atomic step in the path of surface conduction between the L and R probes, we now determine the surface conductivity. From Fig. 2(b), we fitted the potential profiles for the undosed case, before and after the step separately. By extending these functions along the length of the diagonal, we calculated two potential drops which are averaged, giving us a total voltage drop without the step of $\Delta V = (0.110 \pm 0.005)$ V. The total current between the L and R probes was measured to be $I = (4.57 \pm 0.03)$ μA . Equivalently, we fitted the potential profile to the dosed case and obtained a voltage drop of $\Delta V = (0.170 \pm 0.005)$ V and total current $I = (3.25 \pm 0.03)$ μA . For four-probe surface conduction, the sheet conductivity with variable spacing is given by the following formula [13]:

$$\sigma = \frac{I}{2\pi\Delta V} \left(\ln \frac{S_{12} + S_{2R}}{S_{L1}} + \ln \frac{S_{L1} + S_{12}}{S_{2R}} \right) \quad (1)$$

where $S_{\alpha\beta}$ are distance parameters defined in Fig. 1(b) and for our experiments, $S_{L1} = (5 \pm 1)$ μm , $S_{12} = (1.00 \pm 0.01)$ μm and $S_{2R} = (6 \pm 1)$ μm . We obtain $\sigma_c = (2.7 \pm 0.4) \times 10^{-6}$ $\Omega^{-1} \square^{-1}$ from Eq. (1) for the surface without any atomic step in between the L and R probes. This measured

conductivity value is a combination of surface, space charge layer, and bulk conductivities. Incidentally, this value is consistent with those sitting at the higher end of the measured Si-(7×7) sheet conductivity spectrum as discussed above [3,7,8].

To extract a surface conductivity we consider the system before and after dosing. After dosing, the surface state contribution was eliminated and only the space charge layer and bulk contributions remained. Our self-consistent calculations of band bending [20] show that changes to the space charge layer are insignificant after dosing, with a remaining surface state density of $\sim 10^{13}$ cm^{-2} . The Fermi level remains pinned even when dangling bond density is further reduced to 1000 times less than the value corresponding to a clean Si surface, 6×10^{14} cm^{-2} . Therefore, the combined contribution to the overall conductance due to the space charge layer and the bulk remains largely unmodified after dosing. The dosed surface conductivity is obtained from Eq. (1) as $\sigma_d = (1.4 \pm 0.2) \times 10^{-6}$ $\Omega^{-1} \square^{-1}$. The difference between σ_c and σ_d yields the surface conductivity of $\sigma_s = (1.3 \pm 0.3) \times 10^{-6}$ $\Omega^{-1} \square^{-1}$. Note that, using this method, we were able to determine the surface conductivity despite the complexities involved in the analysis of bulk conduction in semiconductors [31–33].

Next, we analyze the tantalizing question: what is the conductivity of a single atomic step? From the undosed (clean) data of Fig. 2(b), the potential jump (marked by an up arrow) is $\Delta V_S = (0.018 \pm 0.005)$ V, and this value is used in Eq. (1) for the parameter ΔV . From the difference between dosed and undosed currents, we obtained the surface current $I = (1.32 \pm 0.03)$ μA . To determine the distance parameter S_{12} [measured normal to the step edge, see Fig. 1(b)], we note Ref. [34] showed altered electronic structure in the vicinity of a step on the 7×7 surface in a region approximately 1.5 nm wide. It is thus reasonable to set $S_{12} = 1.5$ nm since the potential jump at the atomic step should occur across such a distance.

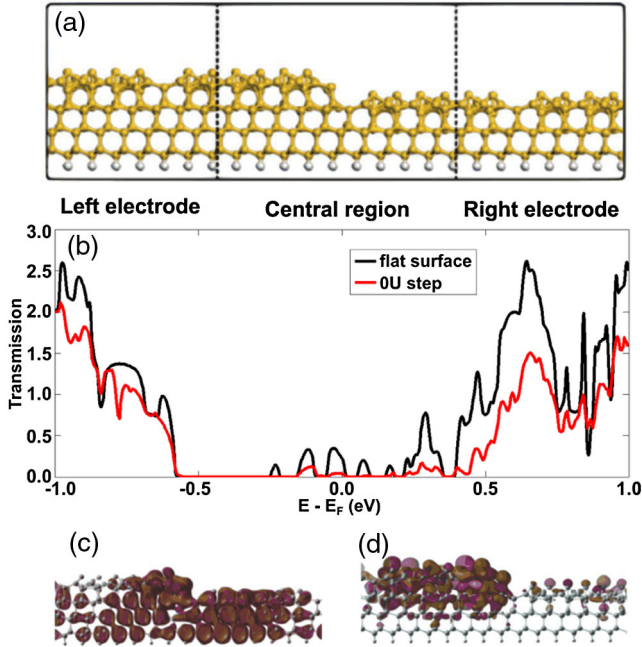


FIG. 3 (color online). (a) Two-probe structure used to calculate electron transport through a step on Si-(7×7). Flat Si-(7×7) surface makes up the electrodes. (b) Transmission spectra of a flat surface and one with an atomic step. Bottom: Scattering states through 0U step. (c) is for the transmission at -0.6 eV, (d) is for the small peak near E_F at -0.03 eV in (b).

Using the model described in Ref. [20], we obtain the atomic step conductivity $\sigma_{\text{step}}^{2\text{D}} = (2 \pm 1) \times 10^{-8} \Omega^{-1} \square^{-1}$. Furthermore, this 2D value can be converted to a 1D barrier conductivity $\sigma_{\text{step}}^{1\text{D}} = 15 \pm 7 \Omega^{-1} \text{m}^{-1}$. Others have suggested that a high density of atomic steps will actually *increase* the surface conductivity [13]. However, in their finite-element calculations, the authors assume that the conductance along an atomic step is 10 times higher than along a perfect 7×7 surface. A direct comparison with our work is not possible since they are considering probe spacings 200 times larger with tens of atomic steps between them [35].

To confirm this model, we have carried out first principles calculations of electron transport along the Si-(7×7) surface with and without a single atomic step. Because of the complexity of this surface there are 14 distinct types of atomic steps possible, as was described by Tochiyama *et al.* [36]. Here we opted to focus on the 0U step type [37]. The atomic positions were relaxed by density functional theory (DFT). The obtained structural and electronic properties are consistent with Ref. [37]. More details can be found in Ref. [20]. The relaxed atomic step structure was then used to construct two-probe transport junctions shown in Fig. 3(a) for electron transport calculations based on the nonequilibrium Green's function technique (NEGF) combined with DFT. The NEGF-DFT method is a well-established formalism for first principles

analysis of charge transport, for details we refer interested readers to Refs. [38–40]. Figure 3(b) compares the transmission spectra for a surface having a single 0U step and another one having no step, which is a flat 7×7 surface having 6 Si layers. The conductance of the system is given by $G = TG_0$ where T is the transmission coefficient and $G_0 = 2e^2/h$ is the conductance quantum. As expected, the transmission through the flat surface without any atomic step (black solid curve) has a significant value near E_F (set at energy zero) [41]. When an atomic step is present on the surface, the calculated transmission inside the band gap is greatly reduced (red curve); this behavior agrees with our experimental observation.

The surface conduction is vividly shown by plotting the calculated wave functions of the scattering states in real space. Scattering states are eigenstates of the open device Hamiltonian connecting the two measuring probes through the scattering region [see Fig. 3(a)]. Two such scattering states (at two different energies) are plotted in Figs. 3(c) and 3(d). Figure 3(c) is a scattering state at energy -0.6 eV which is via the valence band of bulk Si. This wave function is spread throughout the 7×7 slab indicating a large transmission, consistent to that of Fig. 3(b). Figure 3(d) is for a scattering state at the energy just below the E_F and this state does not transmit well to the right electrode indicating a much smaller transmission, also in agreement with Fig. 3(b). Importantly, the scattering state in Fig. 3(d) is predominantly located on the top of the surface and does not penetrate into the bulk layers, confirming the surface conduction in the bulk band gap. Figure 3(d) gives a clear picture of the resistive nature of the atomic step: the amplitude being much smaller for electrons having passed through the step [right side of Fig. 3(d)]. Finally, we have carried out calculations on surfaces with other types of atomic step (0F, 6F, 2U). While these atomic steps give slightly different transmission spectra near E_F , every type reduces transmission at E_F by 3–6 times compared to the step-free surface. Our first principles modeling thus reaches the same conclusion as our experimental measurements, namely, the presence of a single atomic step drastically reduces the overall surface conductance of Si-(7×7).

In summary, we have developed a combined STM and transport measurement technique capable of surface conductivity determination in step-free or single-step containing surface regions and having minimal interaction with the sample, to directly and quantitatively determine the intrinsic conductivity of the Si(111)-(7×7) surface to be $(1.3 \pm 0.3) \times 10^{-6} \Omega^{-1} \square^{-1}$. This is made possible by the capability of measuring the transport property with or without a single atomic step between the voltage probes. In particular, we found that a single atomic step has a conductivity about 50 times smaller per unit length than the flat surface.

We thank Professor Wei Ji for his participation in the early stages of this work and CLUMEQ and RQCHP for

access to computational resources. We are grateful for the able technical assistance of Martin Cloutier and Mark Salomons. This work was supported by NRC, NSERC and iCORE of Canada.

*rwoikow@ualberta.ca

- [1] K. Takayanagi, Y. Tanishiro, M. Takahashi, and S. Takahashi, *J. Vac. Sci. Technol. A* **3**, 1502 (1985).
- [2] B. N. J. Persson, *Phys. Rev. B* **34**, 5916 (1986).
- [3] Y. Hasegawa, I-W Lyo, and Ph. Avouris, *Surf. Sci.* **357–358**, 32 (1996).
- [4] P. G. Piva, G. A. DiLabio, J. L. Pitters, J. Zikovskiy, M. Rezeq, S. Dogel, W. A. Hofer, and R. A. Wolkow, *Nature (London)* **435**, 658 (2005).
- [5] M. Fuechsle, S. Mahapatra, F. A. Zwanenburg, M. Friesen, M. A. Eriksson, and M. Y. Simmons, *Nat. Nanotechnol.* **5**, 502 (2010).
- [6] K. Yoo and H. H. Weitering, *Phys. Rev. B* **65**, 115424 (2002).
- [7] T. Tanikawa, K. Yoo, I. Matsuda, S. Hasegawa, and Y. Hasegawa, *Phys. Rev. B* **68**, 113303 (2003).
- [8] M. D'angelo, K. Takase, N. Miyata, T. Hirahara, S. Hasegawa, A. Nishide, M. Ogawa, and I. Matsuda, *Phys. Rev. B* **79**, 035318 (2009).
- [9] S. Heike, S. Watanabe, Y. Wada, and T. Hashizume, *Phys. Rev. Lett.* **81**, 890 (1998).
- [10] J. W. Wells, J. F. Kallehauge, T. M. Hansen, and Ph. Hofmann, *Phys. Rev. Lett.* **97**, 206803 (2006).
- [11] P. Jachinsky, J. Wensorra, M. L. Lepsa, J. Mysliveek, and B. Voigtlander, *J. Appl. Phys.* **104**, 094307 (2008).
- [12] J. Zikovskiy, Ph.D. thesis, University of Alberta, 2009.
- [13] J. W. Wells, J. F. Kallehauge, and Ph. Hofmann, *Surf. Sci.* **602**, 1742 (2008).
- [14] I. Matsuda, M. Ueno, T. Hirahara, R. Hobara, H. Morikawa, C. Liu, and S. Hasegawa, *Phys. Rev. Lett.* **93**, 236801 (2004).
- [15] Ph. Hofmann and J. W. Wells, *J. Phys. Condens. Matter* **21**, 013003 (2009).
- [16] M. Salomons, B. V. C. Martins, J. Zikovskiy, and R. A. Wolkow, *Rev. Sci. Instrum.* **85**, 045126 (2014).
- [17] M. Ziegler, N. Néel, A. Sperl, J. Kröger, and R. Berndt, *Phys. Rev. B* **80**, 125402 (2009).
- [18] C. Hellenthal, R. Heimbuch, K. Sotthewes, E. S. Kooij, and H. J. W. Zandvliet, *Phys. Rev. B* **88**, 035425 (2013).
- [19] P. Murali and D. W. Pohl, *Appl. Phys. Lett.* **48**, 514 (1986).
- [20] See Supplemental Material at <http://link.aps.org/supplemental/10.1103/PhysRevLett.112.246802> which includes Refs. [21–30], for the theoretical models used in this study and present some extra experimental results.
- [21] G. Kirczenow, P. G. Piva, and R. A. Wolkow, *Phys. Rev. B* **80**, 035309 (2009).
- [22] A. Y. Anagaw, R. A. Wolkow, and G. A. DiLabio, *J. Phys. Chem. C* **112**, 3780 (2008).
- [23] H. Lüth, *Solid Surfaces, Interfaces and Thin Films* (Springer-Verlag, Berlin, 2001).
- [24] G. Kresse and J. Hafner, *Phys. Rev. B* **47**, 558 (1993).
- [25] G. Kresse and J. Furthmüller, *Phys. Rev. B* **54**, 11169 (1996).
- [26] J. P. Perdew, K. Burke, and M. Ernzerhof, *Phys. Rev. Lett.* **77**, 3865 (1996).
- [27] P. E. Blöchl, *Phys. Rev. B* **50**, 17953 (1994).
- [28] G. Kresse and D. Joubert, *Phys. Rev. B* **59**, 1758 (1999).
- [29] M. P. L. Sancho, J. M. L. Sancho, and J. Rubio, *J. Phys. F* **14**, 1205 (1984).
- [30] N. Troullier and J. L. Martins, *Phys. Rev. B* **43**, 1993 (1991).
- [31] E. Perkins, L. Barreto, J. Wells, and P. Hofmann, *Rev. Sci. Instrum.* **84**, 033901 (2013).
- [32] I. Shiraki, F. Tanabe, R. Hobara, T. Nagao, and S. Hasegawa, *Surf. Sci.* **493**, 633 (2001).
- [33] C. M. Polley, W. R. Clarke, J. A. Miwa, M. Y. Simmons, and J. W. Wells, *Appl. Phys. Lett.* **101**, 262105 (2012).
- [34] M. Hupalo, C. Z. Wang, B. J. Min, K. M. Ho, and M. C. Tringides, *Phys. Rev. B* **67**, 115333 (2003).
- [35] We also refer the reader to a related study of a more conductive surface, Si(111)-($\sqrt{3} \times \sqrt{3}$)-Ag, enabling comparison and contrast of the different methods and absolute 2D and 1D conductivities for these surfaces. J. Homoth, M. Wenderoth, T. Druga, L. Winking, R. G. Ulbrich, C. A. Bobisch, B. Weyers, A. Bannani, E. Zubkov, A. M. Bernhart, M. R. Kaspers, and R. Möller, *Nano Lett.* **9**, 1588 (2009).
- [36] H. Tochihara, W. Shimada, M. Itoh, H. Tanaka, M. Udagawa, and I. Sumita, *Phys. Rev. B* **45**, 11332 (1992).
- [37] M. Hupalo, B. J. Min, C. Z. Wang, K. M. Ho, and M. C. Tringides, *Phys. Rev. Lett.* **84**, 2877 (2000).
- [38] M. Smeu, R. A. Wolkow, and H. Guo, *J. Am. Chem. Soc.* **131**, 11 019 (2009).
- [39] J. Taylor, H. Guo, and J. Wang, *Phys. Rev. B* **63**, 245407 (2001).
- [40] D. Waldron, P. Haney, B. Larade, A. MacDonald, and H. Guo, *Phys. Rev. Lett.* **96**, 166804 (2006).
- [41] M. Smeu, H. Guo, W. Ji, and R. A. Wolkow, *Phys. Rev. B* **85**, 195315 (2012).